

pubs.acs.org/Macromolecules Article

Phosphonium-Based Polyzwitterions: Influence of Ionic Structure and Association on Mechanical Properties

Philip J. Scott, Glenn A. Spiering, Yangyang Wang, Zach D. Seibers, Robert B. Moore, Rajeev Kumar, Bradley S. Lokitz, and Timothy E. Long*



Cite This: Macromolecules 2020, 53, 11009–11018



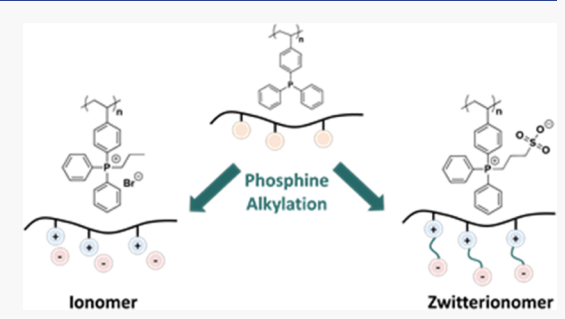
ACCESS

III Metrics & More

Article Recommendations

Supporting Information

ABSTRACT: This manuscript describes a synthetic strategy and structure—property investigation of unprecedented phosphonium-based zwitterionic homopolymers (polyzwitterions) and random copolymers (zwitterionomers). Free radical polymerization of 4-(diphenylphosphino)styrene (DPPS) provided neutral polymers containing reactive triarylphosphines. Quantitative postpolymerization alkylation of these pendant functionalities generated a library of polymers containing various concentrations of neutral phosphines, phosphonium ions, and phosphonium sulfobetaine zwitterions. The zwitterionic homo- and copolymers exhibited significantly higher glass transition temperatures $(T_{\rm g})$ and enhanced mechanical reinforcement in comparison to neutral and phosphonium analogues. These changes in $T_{\rm g}$ and



mechanical properties were attributed to nanoscale morphological domains, which formed due to electrostatic interactions between zwitterionic groups, as revealed by X-ray scattering and broadband dielectric spectroscopy (BDS). BDS revealed increased static dielectric constants (>25) for the phosphonium zwitterionomers compared to ionomeric or neutral analogues. These high static dielectric constants for the solvent-free polyzwitterions supported their stronger polarization response in comparison with polymers containing neutral phosphines and phosphonium ions, and these interactions accounted for morphological differences and enhanced mechanical behavior. This work describes a versatile strategy for modulating electrostatic interactions with tunable mechanical properties for an unprecedented family of zwitterionic polymers.

■ INTRODUCTION

Zwitterions are defined as molecules that contain equal numbers of covalently linked cations and anions, which induce large dipoles (18-30 D for common sulfobetaines)¹ and a net neutral charge. 1,2 Literature studies detail a broad range of zwitterionic structures as small molecules and as functionalities within macromolecular architectures, including diverse combinations of cations (ammoniums, 3 phosphoniums, 4-6 imidazoliums⁷) and anions (carboxylates, sulfonates, sulfates, phosphonates, phosphinates, phosphates).²⁻¹¹ Investigations of zwitterionic small molecules include their use in metal extraction, 12 self-assembled ionic gels and proton conductivity,4 catalytic ligands,6 metal-organic frameworks (MOFs),13 and interfacial materials for solar cells.¹⁴ Literature examples have demonstrated that phosphonium ions impart improved thermal stability and ion conductivity for both small-molecule and polymeric systems compared to ammonium-based analogues. 15,16 Phosphonium zwitterions demonstrate similar advantages; 4,12 however, to the best of our knowledge, the incorporation of phosphonium zwitterions into polymers and copolymers remains unexplored.

Previous literature in this area provides multiple examples of contradictory terminology for zwitterionic polymers, and therefore, this manuscript will invoke the nomenclature as defined in a recent review by Laschewsky.² Polyampholytes are macromolecules that contain both cations and anions covalently bound anywhere within the polymer chain. Polyzwitterions (also termed polybetaines) describe a subclass, which contains the entire zwitterion (cation and anion) within the same repeating unit. In other words, polyzwitterions are polymers containing (usually pendant) functionalities that resemble many of the small-molecule zwitterionic compounds described previously. Zwitterionic dipoles introduce unique functionality to polymers including antimicrobial/anti-biofouling properties,^{9,17} drug conjugation,¹⁸ biomimicry,^{19,20} self-assembly,^{21,22} various stimuli responses,⁸ and thermomechanical reinforcement.^{23,24} The latter arises from the larger dipole moments of zwitterions in comparison to traditional ion pairs due to the separation of charges spatially defined by their covalent linkage. Attractive interactions between antiparallel aligned zwitterions, therefore, offer stronger physical cross-

Received: September 18, 2020 Revised: November 16, 2020 Published: December 3, 2020





linking in zwitterion-containing polymers than similar polyelectrolytes and ionomers. As expected, the strength of these intermolecular interactions is sensitive to temperature and the concentration of added salts, which leads to dramatic changes such as an enhanced solubility in solvents with the addition of salt (also known as the anti-polyelectrolyte effect). For solvent-free environments, previous investigations demonstrated the greater capacity of pendant zwitterions to reinforce polymer thermomechanical properties in comparison to ionomeric analogues. ²³

Synthetic strategies for polyzwitterions explore a range of polymerization and postpolymerization modification techniques to achieve a wide variety of backbone compositions and zwitterionic functionalities.² Typical methods include chainand step-growth polymerizations of zwitterionic monomers, or postpolymerization coupling of zwitterionic substituents onto polymer repeating units.² In addition, alkylation of tertiary amine-containing repeating units with anionic or ionizable ligands generates zwitterionic functionality directly on the polymer. 2,26 Despite a large diversity of polyzwitterion anions, the cation for polyzwitterions remains primarily limited to ammoniums and imidazoliums for their facile synthesis, greater commercial availability, and the relative stability of their corresponding monomers or polymerizable precursors.² To the best of our knowledge, phosphonium cations remain unexplored for polyzwitterions despite promising results for polyampholytes.²⁷ The absence of phosphonium-based zwitterionic monomers and the inherent oxygen sensitivity of typical alkyl phosphine precursors presumably accounts for their omission in the literature.

Previous work in our research laboratories explored triarylphosphine-containing polymers using the commercially available monomer, 4-(diphenylphosphino)styrene (DPPS).^{28–30} The polymers exhibited greater air stability due to the decreased oxygen sensitivity of arylphosphines in comparison to alkylphosphines.³¹ Thus, these polyphosphines served as stable precursors for the subsequent generation of phosphonium-based polyelectrolytes and ionomers upon postpolymerization alkylation. Many earlier literature examples define synthetic approaches to small-molecule phosphonium sulfobetaine zwitterions upon alkylation of triphenylphosphine with sultones, ^{12,32} or alkylation of haloalkylcarboxylic acids with subsequent deprotonation and salt removal.³³ However, these techniques remain unexplored as a synthetic route for phosphonium polyzwitterions.

This manuscript reports the synthesis of the first phosphonium-based polyzwitterions (homopolymers containing zwitterions) and zwitterionomers (random copolymers of zwitterions and other monomers) upon postpolymerization alkylation of DPPS homopolymers and copolymers, respectively. Free radical polymerization of DPPS provided triarylphosphine-containing polymers, which did not readily oxidize at ambient conditions. Quantitative postpolymerization alkylation with sultones and haloalkyl sulfonates installed pendant phosphonium sulfobetaine functionalities, facilitating access to unprecedented phosphonium-based polyzwitterions. Alkylation of the same polyphosphine precursors with alkyl halides yielded phosphonium polyelectrolytes (homopolymer) and ionomers (copolymer) analogues for a systematic structure-property investigation of the neutral, singly charged, and zwitterionic phosphonium-containing polymers. X-ray scattering and broadband dielectric spectroscopy (BDS) analysis provided fundamental insights into the origins of changes in mechanical properties with the introduction of phosphonium-based zwitterionic functionalities.

■ RESULTS AND DISCUSSION

Free radical polymerization of DPPS yielded air-stable, phosphine-containing homopolymers and random copolymers with acrylic monomers. Alkylation of triarylphosphine-containing repeating units with bromopropane yielded phosphonium homopolymers, as illustrated in Scheme 1, and

Scheme 1. Alkylation Strategies for the Synthesis of Phosphonium-Based Polyelectrolytes and Polyzwitterions from polyDPPS Homopolymer Precursors

Phosphonium Sulfobetaine Polyzwitterion

the ring-opening reaction of 1,3-propanesultone with these pendant phosphines yielded salt-free phosphonium sulfobetaines with three methylene spacers between the ion and cation. Shorter zwitterions are known to resist intramolecular cyclization due to contact pair formation and maintain an elongated dipole between charges. ^{34,35}

Molecular weight characterization remains elusive for these polymers due to presumed interactions between the pendant arylphosphines and chromatography columns. However, the use of postpolymerization functionalization strategies enabled a consistent backbone composition and molecular weight distribution among corresponding samples, and direct comparisons between the neutral phosphine, charged phosphonium, and zwitterionic phosphonium sulfobetaine functionalities at each ionic concentration in the polymer.

Many polymer modification reactions generally suffer from limited conversions due to adjacent steric and electronic effects. As a further challenge, previous investigations of small molecule model reactions demonstrated reduced rates of nucleophilic attack of aryl-substituted phosphines. Thus, limited reaction conversions for the alkylation of DPPS-containing polymers were expected and initial studies were critical to determine maximum achievable conversions. PNMR spectroscopy of reaction aliquots monitored phosphine conversion as a function of time for both 1-bromopropane and 1,3-propanesultone alkylations of polyDPPS homopolymers. Despite the aforementioned challenges, the quantitative

conversion of the phosphine as a pendant substituent in each repeating unit was quantitative for both alkylation pathways, as determined within the detection limit of ³¹P-NMR spectroscopy (Figure 1). However, as expected for triarylphosphino

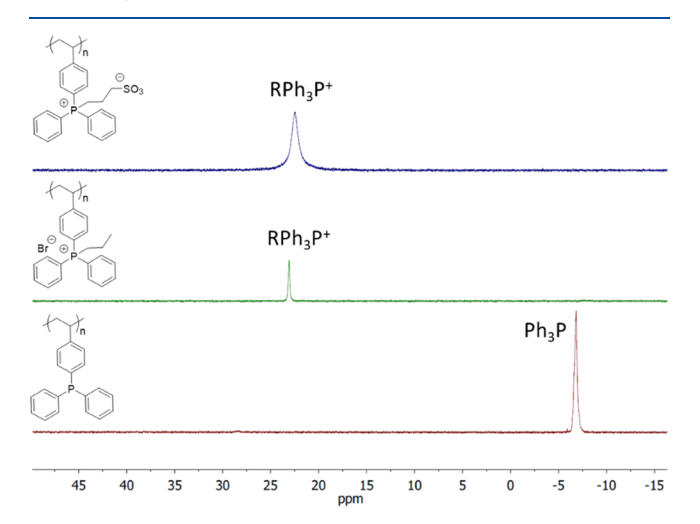


Figure 1. Quantitative postpolymerization alkylation of polyDPPS homopolymers yields both ionomers and polyzwitterions, as confirmed by ³¹P NMR spectroscopy. DMSO-*d*₆.

nucleophiles, the reaction rates were sluggish with required reaction times of 1-2 weeks. Apparent plateaus in phosphine conversion with respect to time were often observed; however, this was attributed to the loss of alkylation reagents, e.g., sultone hydrolysis. These limited conversions were overcome with the further addition of alkylation reagent and allowing additional time for the complete disappearance of the phosphine peak (-6.8 ppm) with the formation of a phosphonium peak at 22.5 ppm in deuterated DMSO.

Alkylation of polyDPPS homopolymers confirmed the possibility of quantitative conversion of polymeric triarylphosphines; however, both the neutral and the alkylated

homopolymers produced extremely brittle films. This precluded these polymers as candidates for further mechanical studies to establish structure—property relationships. Scheme 2 illustrates the copolymerization of DPPS with di(ethylene glycol)methyl ether methacrylate (DEGMEMA), which led to a lower glass transition temperature, and consequently, improved mechanical integrity was attained for random copolymers with varying concentrations of phosphine functionality, i.e., 5, 10, and 31 mol % (7, 15, 41 wt % DPPS). In a similar approach as before, the poly(DPPS-co-DEGMEMA) copolymers served as a common precursor for alkylation and ensured consistency in molecular weight, dispersity, and backbone composition between the neutral, ionic, and zwitterionic copolymers at each composition.

Alkylation of these random copolymers yielded phosphonium ionomers and zwitterionomers with systematic variation in the ion concentration. The alkylations proceeded similarly to the homopolymer, exhibiting slow reaction kinetics and nearly quantitative phosphine conversion for all samples within 1-2 weeks. The conversions were confirmed with a shift from the phosphine peak (-6.8 ppm) to the phosphonium peak (23.3 ppm), as shown in Figure 2. Low levels of oxidation (as confirmed with a peak at 24.9 ppm) appeared for the lower mol % phosphine samples, presumably due to the introduction of low levels of atmospheric oxygen during the long reaction time. Interestingly, additional peaks around the Ph₃P peak are seen for the neutral samples, possibly due to the presence of different environments for the phosphine within the random copolymer backbone. This is supported by the lack of these additional peaks in the homopolymer (Figure 1); however, this observation warrants further investigation. The resulting polymer library enabled systematic investigation into the influences of ionic composition and molar concentrations on polymer properties.

All copolymers exhibited single T_g s, as observed with differential scanning calorimetry (DSC). The T_g of the neutral poly(DPPS-co-DEGMEMA) copolymers increased upon

Scheme 2. Free Radical Copolymerization of DPPS and DEGMEMA Yields Phosphine-Containing Random Copolymers^a

^aSubsequent alkylation with an alkyl halide or sultone reagents generates phosphonium ionomers and zwitterionomers, respectively.

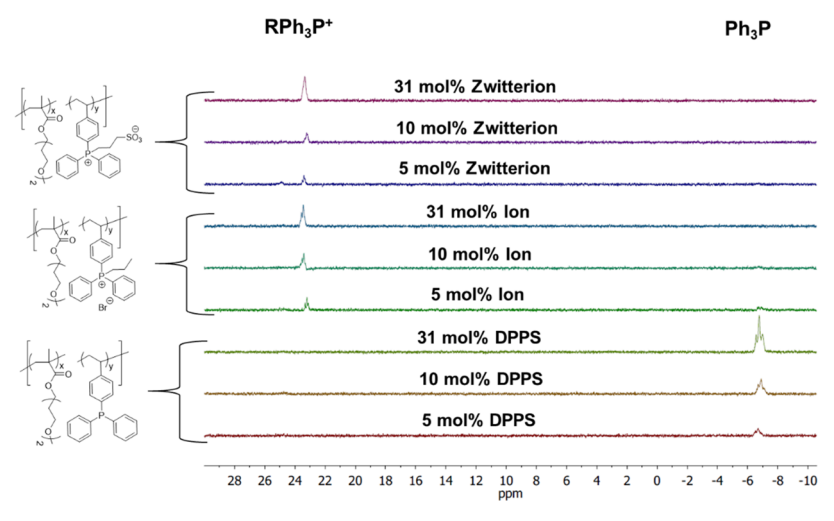


Figure 2. Alkylation of poly(DPPS-co-DEGMEMA) copolymers yields both phosphonium ion and zwitterion functionalities, as confirmed by ^{31}P NMR spectroscopy. DMF- d_7 .

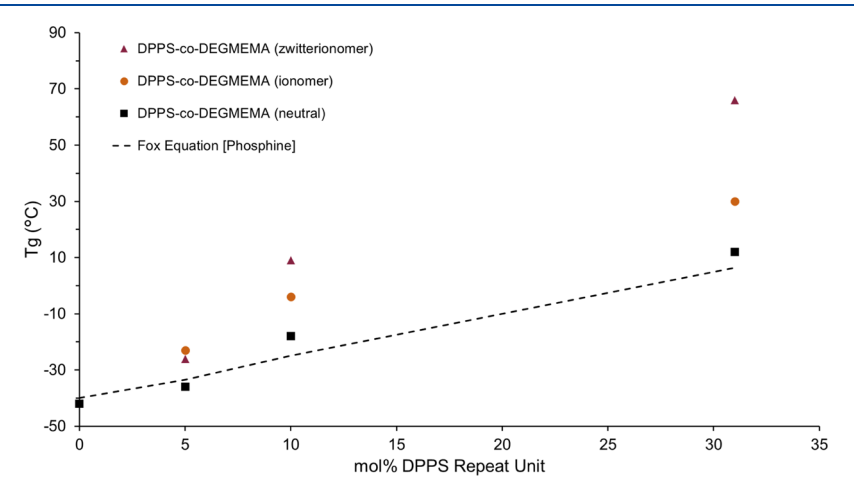


Figure 3. Effect of DPPS incorporation and alkylation state on glass transition temperature (T_g) , as measured by differential scanning calorimetry (DSC). $T_g = 118$ °C of the polyDPPS homopolymer was calculated using the Fox equation.

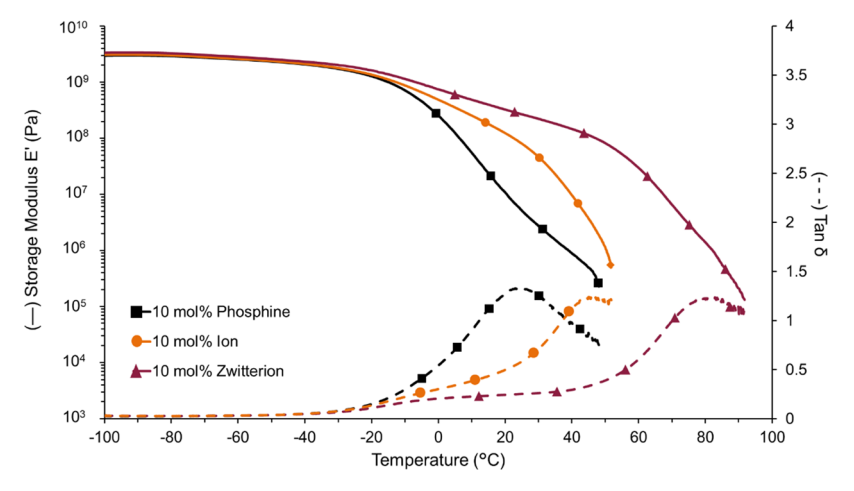


Figure 4. Increased reinforcement by ionic and zwitterionic functionalities, as confirmed by DMA and evidenced by an extension of the tensile storage modulus (E') rubbery plateau (solid lines) to higher temperatures. Loss tangent $(\tan \delta)$ lines represented as dashed lines.

DPPS incorporation and closely aligned with the prediction of the Fox equation, suggesting random copolymerization of DEGMEMA (homopolymer $T_{\rm g} = -40~^{\circ}{\rm C})^{36}$ and DPPS (homopolymer $T_{\rm g} = 118~^{\circ}{\rm C}$), as shown in Figure 3. Bocharova et al., Matsurra et al., and Eisenberg et al. have reported

increases in $T_{\rm g}$ with increasing ion content due to the restriction of cooperative backbone segmental motion attributed to electrostatic interactions between ionomeric chains. ^{37–40} Phosphonium ionomers exhibited similar behavior, and $T_{\rm g}$ s increased relative to the neutral polyphosphine

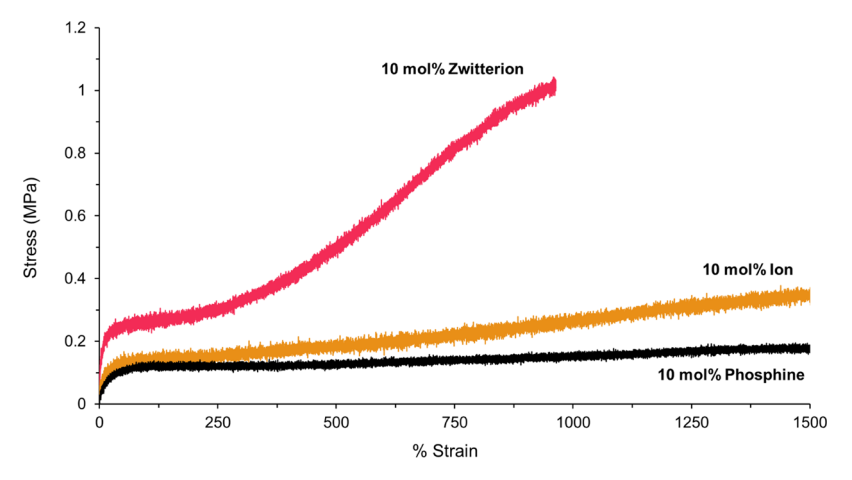


Figure 5. Tensile analysis of 10 mol % DPPS samples demonstrated significant mechanical reinforcement by the zwitterionic functionalities. Dogbones die-cut with an ASTM D-638V punch and subjected to tensile analysis, which was performed on an Instron 5500 at room temperature at a strain rate of 5 mm/min. Only the 10 mol % zwitterion sample broke during testing.

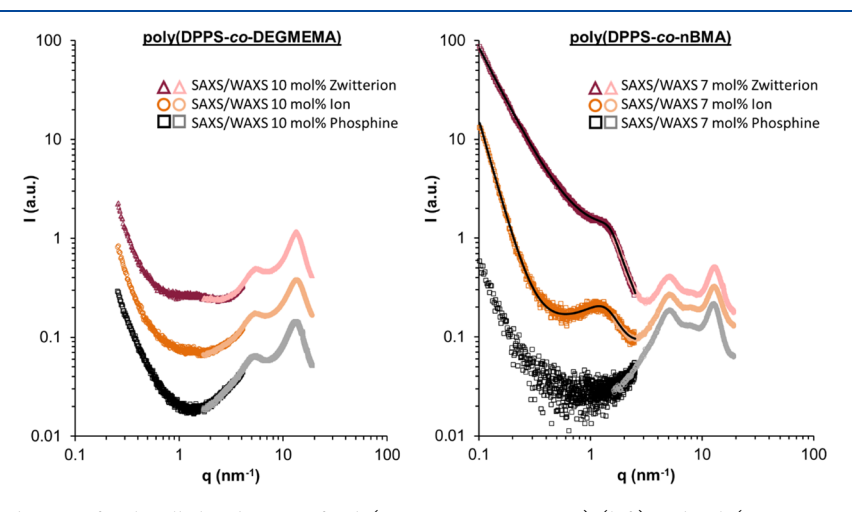


Figure 6. Presence of ionic domains for the alkylated states of poly(DPPS-co-DEGMEMA) (left) and poly(DPPS-co-nBMA) (right), as confirmed by combined SAXS/WAXS. Line overlays in the right plot show Kinning—Thomas model fitting. All curves are vertically shifted for clarity.

precursor at each molar concentration in the copolymer. Zwitterions provide larger dipoles than contact ion pairs due to the charge separation imposed by the covalent attachment between each ion. Previous work elucidated the head-totail anti-parallel alignment of zwitterionic dipoles, although energetically less favorable, to provide strong physical interactions between them. These large dipoles as a result yield stronger physical crosslinking in phosphonium polyzwitterions with greater $T_{\rm g}$ increases than the corresponding ionomeric copolymers, shown in Figure 3. Furthermore, the degree of $T_{\rm g}$ enhancement increased with molar concentration in the copolymer, further supporting the dramatic influence of these electrostatic interactions on thermal properties. These observations aligned with similar investigations of ammonium-based ionomers and zwitterionomers.

In addition to increasing $T_{\rm g}$, the physical intermolecular crosslinking due to (zwitter)ionic interactions manifested as reinforcement of mechanical properties. Dynamic mechanical analysis (DMA) was used to compare the tensile storage modulus (E') and loss tangent ($\tan\delta$) of copolymer films with 10 mol % phosphine, phosphonium ion, and phosphonium sulfobetaine zwitterion functionalities (Figure 4). The neutral phosphine copolymer exhibited flow at temperatures above $T_{\rm g}$ due to the lack of physical crosslinking beyond entanglements.

Physical reinforcement upon the incorporation of ionic and zwitterionic interactions extended the tensile storage modulus (E'), providing a plateau E' to temperatures above $T_{\rm g}$. In agreement with the $T_{\rm g}$ trends observed previously, the stronger physical crosslinking within the zwitterionomer sample yielded greater reinforcement of the E' plateau to higher temperatures than the ionomer at the same molar concentration in the copolymer.

Tensile analysis, as depicted in Figure 5, provided further evidence for the unique capability of zwitterions to reinforce polymers and offered insight into the mechanical performance of zwitterionic copolymers. As expected, the low $T_{\rm g}$, noncrosslinked neutral copolymer (10 mol % phosphine) exhibited very low maximum stresses (<0.2 MPa) upon elongation and plastically deformed to high strains without breakage. While the presence of ionic physical crosslinking in the phosphonium ionomer (10 mol %) increased stress upon deformation, plastic deformation remained due to the breakage and reforming of ionic associations (i.e., "ion hopping").39 Stress appeared to increase at higher strains, possibly indicating additional ionic aggregation facilitated by alignment and sliding of polymer chains. The zwitterionomer exhibited dramatically increased stress upon elongation with an ultimate strength above 1 MPa due to the stronger physical crosslinking between chains and

displayed significant strain-hardening upon deformation to high strains. Middleton et al. correlated strain-hardening of ionomers to deformation-induced morphological changes in the ionic aggregates. Similar morphological changes may explain the strain-hardening observed for these copolymers, which warrants further study.

Small-angle (SAXS) and wide-angle X-ray scattering (WAXS) measurements confirmed the presence of ionic aggregation in both the phosphonium ionomer and phosphonium sulfobetaine zwitterionomer polymers (Figure 6). In particular, strong electrostatic interactions in solvent-free charged polymers are expected to manifest as peaks at finite wavevectors in the SAXS for the ionomer and polyzwitterion states (similar to those observed in Figure 6). Wavevectors at the peaks have been shown to be dependent on an electrostatic interaction parameter proportional to the Bjerrum length (in vacuum) times the square of the dipole moment.⁵⁰ However, in-depth analysis of these peaks for the DEGMEMA-based copolymers proved challenging, presumably due to poor contrast. Synthesis of similar copolymers with the alkyl monomer, n-butyl methacrylate (nBMA), appeared to provide improved contrast and displayed well-defined peaks suitable for fitting with the Kinning-Thomas model (Table 1).

Table 1. Kinning—Thomas Fitting Parameters for poly(DPPS-co-nBMA) Copolymer Series

poly(DPPS-co-nBMA)	R_1 (nm)	$R_{\rm ca} \ ({\rm nm})$	$v_p (nm^3)$
7 mol % ion	1.49 ± 0.03	2.03 ± 0.03	230 ± 12
7 mol % zwitterion	1.81 ± 0.02	1.92 ± 0.01	120 ± 3

Alkylation with bromopropane generated a direct analogue to the DEGMEMA-based phosphonium ionomer (Scheme S1). Alkylation of poly(DPPS-co-nBMA) with bromopropane sulfonate explored a less hazardous, sultone-free route to zwitterion formation. It is important to note that unlike sultone ring-opening, alkylation with bromopropane sulfonate does not necessarily preclude the presence of sodium and bromide counterions for the sulfonate and phosphonium, respectively. However, Romanov and co-workers reported the synthesis of small-molecule phosphonium carboxybetaines, which utilized aqueous conditions to remove sodium bromide salts after alkylation.³³ Therefore, polyzwitterions synthesized through

this approach required thorough aqueous washing with liquid—liquid extraction of the reaction solution.

The excess scattering centered around 1.40 nm⁻¹ for the ionic and zwitterionic species of the poly(DPPS-co-DEGME-MA) series implied the presence of some weak, disordered phase separation to yield ionic domains. However, prominent ionic domain peaks appeared for the alkylated polymers in the poly(DPPS-co-nBMA) series. For both copolymer series, the amount of phase separation appeared to increase with increasing intermolecular interactions from phosphine to ionic to zwitterion. SAXS scattering profiles were fit using a liquid-like hard-sphere model according to Kinning and Thomas⁵¹ (Table 1), following a formulation for the SAXS modeling interference terms (structure factors) defined by Winey et al.⁵² These fits provided quantitative insights concerning the size and spacing of the ionic domains. The liquid-like hard-sphere model describes collections of aggregates with respect to three principal spatial parameters (cf. Table 1): the radius of the spherical aggregate (R_1) , the radius of the closest approach (R_{ca}) , and the sample polymer volume per ionic aggregate (V_p) . The zwitterionic species tended to have a higher R_1 than the ionic series and lower V_p . This result therefore indicated a greater volume fraction $(=(4/3)*\pi*R_1^3/$ $V_{\rm p}$) occupied by domains of larger radii present for the zwitterionic series compared to the ionic series. Although the Kinning-Thomas model is useful for extracting quantitative information about sizes and distribution of domains appearing in limited regions in the SAXS, the model does not provide a molecular description for the existence of the domains revealed by peaks at intermediate wavevectors and cannot be used to explain enhanced scattering observed at lower wavevectors. In this work, we have used an ad hoc background term to fit excess scattering at lower wavevectors. Macromolecular models⁵⁰ considering effects of electrostatics need to be considered to interpret additional features seen in the SAXS and WAXS. Detailed analysis of the scattering data using molecular models will be presented in future work. Based on our preliminary analysis and other related works from the literature, 35,53 peaks seen in the WAXS can be assigned to the two types of side-chains (DEGMEMA and functionalized DPPS) in these copolymers (see Figures S8 and S9 showing the location of these peaks for the DEGMEMA-based copolymers). The number of ions per aggregate can be

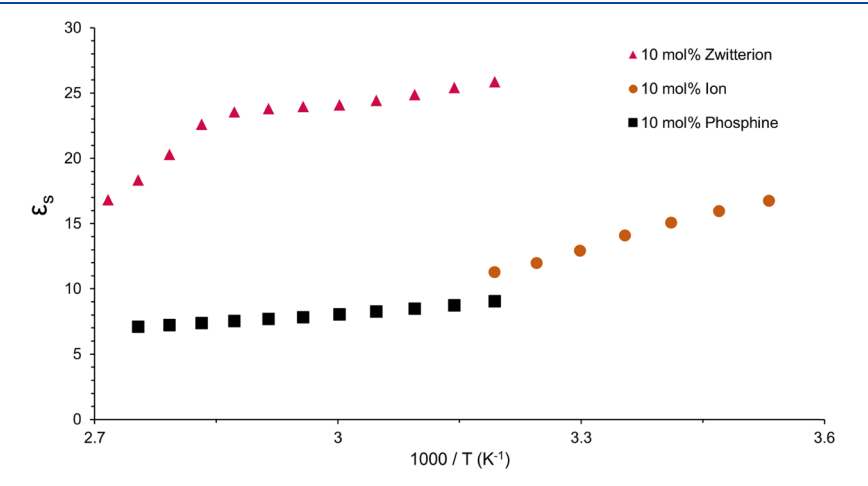


Figure 7. Static dielectric constants (ε_s) calculated from BDS for poly(DPPS-co-DEGMEMA) random copolymers with 10 mol % neutral phosphine, phosphonium ion, and phosphonium sulfobetaine zwitterion functionalities.

estimated by assuming space-filling of a spherical aggregate domain by monomers (containing cations and anions), whose size is estimated to be \sim 0.45 nm using WAXS results (cf. Figure S9). These considerations lead to the number of ions per aggregated domain to be $(R_1/0.45)^3$, which turns out to be $(1.49/0.45)^3 \sim 36$ and $(1.81/0.45)^3 \sim 65$ for 7% ion and zwitterion, respectively. Hence, the number of ions per aggregate turns out to be higher for the zwitterionomer than the ionomer pointing out stronger attractive interactions in the zwitterionomer.

Experimental results related to thermomechanical properties and scattering are consistent with stronger attractive intra- and intermolecular interactions in the zwitterionomers than the ionomers and the neutral polymers. The molecular origin of such interactions is expected to be the zwitterions acting as stronger electric dipoles than the contact ion-pairs present in the ionomers. To verify this expectation, we employed broadband dielectric spectroscopy (BDS) to estimate the static dielectric constants (ε_s) of polyphosphine, phosphonium ionomer, and phosphonium zwitterionomer (10 mol %). These values, shown in Figure 7, correlate to the concentration and dipole moment (μ) of dipoles present in the polymer via the Onsager–Kirkwood formula (eq 1). $^{54-56}$

$$\frac{(\varepsilon_{\rm s}-1)(2\varepsilon_{\rm s}+1)}{\varepsilon_{\rm s}} = \frac{4\pi\beta N\mu^2 g_{\rm K}}{\Omega} \tag{1}$$

where β is the inverse of the Boltzmann constant times temperature, N is the number of dipoles in the system of volume Ω . g_K is the Kirkwood g-factor that describes orientation correlations of the dipoles. Due to the presence of polar groups in the DEGMEMA and uncharged DPPS monomers, the polyphosphine exhibited dielectric constants on the order of 7 at the experimental temperatures, which were relatively high in comparison to other neutral polymers (e.g., ε = 2.5 for polystyrene⁵⁷). The incorporation of phosphonium ions increased these values, either due to the enhanced polarizability of the ions or the introduction of phosphonium bromide ion pairs. The zwitterionomer exhibited significantly higher static dielectric constants than the ionomer and polyphosphine, confirming the presence of stronger dipoles due to the zwitterionic functionalities. It is important to note that all alkylations occurred on fractions of the same polyphosphine precursor so that the overall concentration of phosphonium ions was identical for the ionomer and the polyzwitterion. Thus, the significant increase in ε_s suggested significantly higher μ values for the pendant zwitterions and supported the role of zwitterionic interactions in the considerable increases in $T_{\rm g}$ and (thermo)mechanical reinforcement observed for the phosphonium zwitterionomers.

CONCLUSIONS

Polymerization of a triarylphosphine monomer enabled polymeric precursors, which yielded the first examples of phosphonium-based polyzwitterions and zwitterionomers upon sultone alkylation. ³¹P-NMR spectroscopy confirmed near-quantitative conversions of pendant phosphines for both homopolymers and random copolymers despite long reaction times. A systematic investigation between the neutral phosphine, phosphonium ionomer, and phosphonium sulfobetaine zwitterionomer yielded insights into the greater physical crosslinking between pendant zwitterionic dipoles compared to ionomer analogues, evidenced by considerable

increases in T_g , storage modulus, and stress upon elongation, as detailed in Table 2. Furthermore, the phosphoniosulfobetaine

Table 2. Thermal, Mechanical, and Dielectric Data for 10 mol % Copolymer Series

	T _g < < (C)	E' @ 20 °C (MPa)	stress @ 100% strain (MPa)	stress @ 500% strain (MPa)	ε _s @ 40 °C
10 mol % phosphine	-18	11	0.11	0.13	9
10 mol % ion	-4	123	0.15	0.19	11
10 mol % zwitterion	9	327	0.26	0.50	26
^a Measured b	by DSC.				

dipoles enabled a nearly 3-fold increase in the static dielectric constant determined by BDS and ionic domains observed by SAXS supported the role of zwitterionic interactions to strongly direct and reinforce (thermo)mechanical properties. This study stages multiple new research directions focused on the fundamental and applied aspects related to the structure and dynamics of phosphonium-containing polyzwitterions and zwitterionomers.

EXPERIMENTAL SECTION

Materials. 4-(Diphenylphosphino) styrene (DPPS), di(ethylene glycol) methyl ether methacrylate (DEGMEMA), *n*-butyl methacrylate (*n*BMA), bromopropane, and 1,3-propanesultone were purchased commercially from Sigma-Aldrich and used directly without further purification. Azobisisobutyronitrile (AIBN) was purchased from Sigma Aldrich and recrystallized from methanol prior to use. Anhydrous dimethylformamide (DMF) for alkylation reactions was purchased from Sigma Aldrich. All other solvents were purchased as HPLC grade from Fisher Scientific and used directly.

Synthesis of DPPS Homopolymers and Copolymers. The following provides an example polymerization of a polyDPPS homopolymer. In a 100-mL round-bottomed flask, 5 g of DPPS and 17 mg of AIBN (0.6 mol %) were dissolved in 20 mL CHCl₃. The reaction solution was sparged with argon for 20 min before heating in an oil bath to 65 °C for 16 h. The reaction solution was then cooled to room temperature, concentrated via rotary evaporation, and precipitated from diethyl ether three times. The polymer was then dried *in vacuo* at room temperature for 24 h.

The following provides an example polymerization of poly(DPPS-co-DEGMEMA). In a 100-mL round-bottomed flask, 1 g of DPPS, 9 g of DEGMEMA, and 24 mg of AIBN (0.6 mol %) were dissolved in 60 mL of chloroform. The solution was sparged with argon for 20 min while stirring before heating in an oil bath to 65 °C for 16 h. The reaction was cooled to room temperature, and the product solution was concentrated via rotovaporization and dialyzed (3.5 kDa, snakeskin) against chloroform to remove the residual starting material. The polymer was then precipitated from the dialyzed chloroform solution in methanol and dried *in vacuo* at room temperature for 24 h. Synthesis and purification of nBMA copolymers followed this same procedure.

Postpolymerization Alkylation of DPPS-Containing Polymers. In an example alkylation, 1.25 g of polymer was dissolved in 20 mL of dimethylformamide (DMF) in a 50 mL round-bottomed flask. The solution was sparged with argon for 20 min before adding 3 equiv (with respect to phosphine repeat units) of either bromopropane or 1,3-propanesultone using a syringe. The reactions were heated to 65 °C (bromopropane) or 90 °C (sultone), determined by the boiling point of the bromopropane. It is important to note that 1,3-propanesultone is a uniquely potent human carcinogen that demands extreme caution during handling. See Conversion of the pendant triarylphosphines was monitored via 31P-NMR spectroscopy. If

Table 3. SAXS Fitting Parameters for DPPS-co-nBMA Series

poly(DPPS-co-nBMA)	R_1	R_{ca}	\mathbf{v}_{p}	a_1	a_2	k	d
7 mol % ion	1.49 ± 0.03	2.03 ± 0.03	230 ± 12	0.0491 ± 0.0119	0.0119 ± 0.0047	0.00122 ± 0.00005	1.96 ± 0.02
7 mol % zwitterion	1.81 ± 0.02	1.92 ± 0.01	120 ± 3	0.467 ± 0.019	-0.146 ± 0.008	0.230 ± 0.003	3.76 ± 0.01

conversion progress appeared to plateau, additional alkylation agent (3 equiv) was added using a syringe. In this manner, reactions were continued until full phosphine conversion was observed. Upon completion, the sultone reactions were allowed to cool to room temperature and 1 mL of water was added to quench any residual sultone. Water was also used through the process to quench all equipment that contacted sultone. Reaction solutions were then directly dialyzed against methanol to remove DMF solvent and residual alkylation reagent. The dialyzed methanol solutions were then poured into poly(tetrafluoroethylene) (PTFE) molds dishes (6 cm diameter) for solvent removal and film preparation.

Alkylation of poly(DPPS-co-nBMA) to the ionomer state proceeded as described above. The polymer was dialyzed against CHCl₃, and the dialysate was concentrated via rotovaporization and poured into a PTFE mold for drying and film preparation. Alkylation for zwitterions of nBMA copolymers utilized bromopropane sodium sulfonate in lieu of 1,3-propanesultone but otherwise followed the same reaction conditions. After completion, the poly(DPPS-co-nBMA) polyzwitterion reaction solution was diluted in CHCl₃ and the solution was washed via liquid—liquid extraction with water three times. The organic layer was collected, concentrated via rotovaporization, and cast into a PTFE mold for drying and film preparation.

Film Preparation via Solvent-Casting. Unalkylated DPPS (phosphine)-based polymers were solution-casted as 20 wt % solutions in chloroform. Alkylated homopolymers and alkylated DEGMEMA copolymers (phosphonium ion and zwitterion) were casted as solutions in methanol (from dialysis or prepared as 20 wt % solutions). In either case, the dry polymer mass for each sample was approximately 1 g. Polymer solutions were poured into PTFE molds (6 cm diameter) and covered with a glass cover dish (propped with a paper clip to allow low air flow) on the benchtop. After 12 h, the PTFE dishes were moved to the vacuum oven at room temperature for 12 h, and then increased to 65 °C for 24 h. After drying, the films were then removed from the dishes, placed onto PTFE film, and stored in a desiccator.

Analysis of Polymer Array. ¹H- (64 scans, 5 s relaxation delay) and ³¹P-NMR spectroscopy (64 scans, 25 s relaxation delay) was used to confirm monomer and polymer chemical compositions and phosphorous state (phosphine [-6.8 ppm], phosphonium [23.3 ppm], phosphine oxide [24.9 ppm], DMF- d_7). Thermogravimetric analysis (TGA) was performed at a ramp rate of 10 °C/min with a 20 min isotherm drying step at 120 °C. Differential scanning calorimetry (DSC) was run at 10 °C/min heating/cooling rate in a heat—cool—heat cycle and polymer and copolymer thermal properties were determined. T_g values were determined from the DSC curve inflection half-height via TA TRIOS software. Dogbones were die-cut with an ASTM D-638V punch and subjected to tensile analysis, which was performed on an Instron 5500 at room temperature at a strain rate of 5 mm/min.

Broadband Dielectric Spectroscopy (BDS). Broadband dielectric spectroscopy measurements were carried out with a Novocontrol Concept 40 system, consisting of an Alpha-A impedance analyzer, a ZGS test interface, and a QUATRO cryosystem, in the frequency range $0.1-10^7$ Hz and temperature range 120 to -60 °C. In each experiment, a disk-shaped sample was sandwiched between two gold-plated electrodes, and a Teflon ring spacer of $125~\mu m$ in thickness was used to maintain a constant gap. To remove any residual solvent or absorbed water, the sample was first equilibrated at 120 °C for several hours until the dielectric spectrum no longer changed with time. We note that the real permittivity of these samples is not completely flat in the low-frequency region before electrode polarization (see Figure S10). Therefore, to extract the static dielectric permittivity ϵ_{sy} nonlinear least-squares analysis was employed to simultaneously fit

the real, imaginary, and derivative dielectric spectra, using a phenomenological model of the following form $\epsilon^*(\omega) = \frac{\sigma}{i\epsilon_0\omega} + \sum_j \frac{\Delta\epsilon_j}{[1+(i\omega\tau_j)^{\alpha_j}]^{\beta_j}} + \epsilon_\infty + A\omega^{-n}. \text{ Here, } \omega = 2\pi f \text{ is the }$

angular frequency, ϵ_{∞} is the value of ϵ' at "infinite" frequency, $\Delta \epsilon_{j}$ is the dielectric relaxation strength, τ_{j} is the relaxation time, α_{j} and β_{j} are the shape parameters, and σ is the dc conductivity (see Figure S11). A total of two Havriliak–Negami terms were used in the fitting. The static permittivity ϵ_{s} was calculated as $\epsilon_{s} = \epsilon_{\infty} + \Delta \epsilon_{1} + \Delta \epsilon_{2}$. Understanding the microscopic origin of dielectric relaxation in these copolymers requires further systematic study, which we plan for future work.

X-ray Scattering Analysis. Small-angle X-ray scattering (SAXS) and wide-angle X-ray scattering (WAXS) experiments were performed using a Rigaku S-Max 3000 3 pinhole SAXS system, equipped with a rotating anode emitting X-ray with a wavelength of 0.154 nm (Cu $K\alpha$). The sample-to-detector distance was 1005 or 1600 mm for SAXS and 195 mm for WAXS, and the q-range was calibrated using a silver behenate standard. Two-dimensional SAXS patterns were obtained using a 2D multiwire, proportional counting, gas-filled detector, with an exposure time of 2 h. Two dimensional WAXS diffraction patterns were obtained using an image plate with an exposure time of 1 h. The SAXS data were corrected for sample thickness, transmission, and background, and were put on an absolute scale by correction using a glassy carbon standard from the Advanced Photon Source (APS). The WAXS data were corrected for background. The SAXS/WAXS profiles were vertically shifted to facilitate a comparison of peak positions. All of the SAXS and WAXS data were analyzed using the SAXSGUI software package to obtain radially integrated SAXS and WAXS intensity versus the scattering vector q (SAXS) or 2θ (WAXS), respectively, where $q=(4\pi/2)^{1/2}$ λ)sin(θ), θ is one-half of the scattering angle, and λ is the X-ray wavelength. For fitting the SAXS data, scattering intensity based on the Kinning-Thomas model^{49,50} was complemented with an additional term of the form $a_1 + a_2 q + \frac{k}{q^{6-d}}$. The additional term was particularly useful for fitting the scattering at lower wavevectors.

The fit results are found in Table 3.

ASSOCIATED CONTENT

Supporting Information

The Supporting Information is available free of charge at https://pubs.acs.org/doi/10.1021/acs.macromol.0c02166.

 1 H and 31 P NMR spectra of poly(DPPS-co-DEGME-MA) copolymers; fitting examples for BDS data; synthetic scheme and 31 P NMR spectra poly(DPPS-co-nBMA) copolymers; SAXS/WAXS plots for both copolymer series; plots of WAXS peak location and d spacing with respect to DPPS concentration in the polymer; plot of ε' (from BDS) with respect to frequency; plot of ionic conductivity (from BDS) with respect to 1000/T; DSC curves for poly(DPPS-co-DEGMEMA) series (PDF)

AUTHOR INFORMATION

Corresponding Author

Timothy E. Long – School of Molecular Sciences, Biodesign Center for Sustainable Macromolecular Materials and Manufacturing (BCSM3), Arizona State University, Tempe,

Arizona 85281, United States; o orcid.org/0000-0001-9515-5491; Email: telong@asu.edu

Authors

- Philip J. Scott Department of Chemistry, Macromolecules Innovation Institute, Virginia Tech, Blacksburg, Virginia 24061, United States; oorcid.org/0000-0002-4219-6000
- Glenn A. Spiering Department of Chemistry, Macromolecules Innovation Institute, Virginia Tech, Blacksburg, Virginia 24061, United States
- Yangyang Wang Center for Nanophase Materials Sciences, Oak Ridge National Laboratory, Oak Ridge, Tennessee 37830, United States; oorcid.org/0000-0001-7042-9804
- Zach D. Seibers Center for Nanophase Materials Sciences, Oak Ridge National Laboratory, Oak Ridge, Tennessee 37830, United States; orcid.org/0000-0001-9749-4307
- Robert B. Moore Department of Chemistry, Macromolecules Innovation Institute, Virginia Tech, Blacksburg, Virginia 24061, United States; orcid.org/0000-0001-9057-7695
- Rajeev Kumar Center for Nanophase Materials Sciences and Computational Sciences and Engineering Division, Oak Ridge National Laboratory, Oak Ridge, Tennessee 37830, United States; orcid.org/0000-0001-9494-3488
- Bradley S. Lokitz Center for Nanophase Materials Sciences, Oak Ridge National Laboratory, Oak Ridge, Tennessee 37830, United States; orcid.org/0000-0002-1229-6078

Complete contact information is available at: https://pubs.acs.org/10.1021/acs.macromol.0c02166

Notes

The authors declare no competing financial interest.

■ ACKNOWLEDGMENTS

A portion of this research related to synthesis, BDS, and data analysis was conducted at the Center for Nanophase Materials Sciences, which is a DOE Office of Science User Facility at Oak Ridge National Laboratory. This is also based upon work supported by the National Science Foundation under Grant No. DMR-1809291. The authors also thank Dr. Mingtao Chen for helpful discussions and his expertise with ionomers and polyionic liquids.

REFERENCES

- (1) Galin, M.; Chapoton, A.; Galin, J.-C. Dielectric Increments, Intercharge Distances and Conformation of Quaternary Ammonioal-kylsulfonates and Alkoxydicyanoethenolates in Aqueous and Tirfluoroethanol Solutions. *J. Chem. Soc., Perkin Trans.* 2 1993, 545–553.
- (2) Laschewsky, A. Structures and Synthesis of Zwitterionic Polymers. *Polymers* **2014**, *6*, 1544.
- (3) Saita, S.; Mieno, Y.; Kohno, Y.; Ohno, H. Ammonium Based Zwitterions Showing Both LCST- and UCST-Type Phase Transitions after Mixing with Water in a Very Narrow Temperature Range. *Chem. Commun.* **2014**, *50*, 15450–15452.
- (4) Ueda, S.; Kagimoto, J.; Ichikawa, T.; Kato, T.; Ohno, H. Anisotropic Proton-Conductive Materials Formed by the Self-Organization of Phosphonium-Type Zwitterions. *Adv. Mater.* **2011**, 23, 3071–3074.
- (5) Geier, S. J.; Dureen, M. A.; Ouyang, E. Y.; Stephan, D. W. New Strategies to Phosphino–Phosphonium Cations and Zwitterions. *Chem. Eur. J.* **2010**, *16*, 988–993.
- (6) Pews-Davtyan, A.; Jackstell, R.; Spannenberg, A.; Beller, M. Zwitterionic Phosphonium Ligands: Synthesis, Characterization and Application in Telomerization of 1,3-Butadiene. *Chem. Commun.* **2016**, *52*, 7568–7571.

- (7) Hajishaabanha, F.; Shaabani, S.; Shaabani, A.; Sangachin, M. H.; Dusek, M.; Kučeráková, M. Synthesis of Imidazolium Zwitterions via an Efficient One-Pot Three-Component Synthetic Protocol. *J. Iran. Chem. Soc.* **2020**, *17*, 513–519.
- (8) Ilčíková, M.; Tkáč, J.; Kasák, P. Switchable Materials Containing Polyzwitterion Moieties. *Polymers* **2015**, *7*, 2344–2370.
- (9) Tada, S.; Inaba, C.; Mizukami, K.; Fujishita, S.; Gemmei-Ide, M.; Kitano, H.; Mochizuki, A.; Tanaka, M.; Matsunaga, T. Anti-Biofouling Properties of Polymers with a Carboxybetaine Moiety. *Macromol. Biosci.* **2009**, *9*, 63–70.
- (10) Hamaide, T.; Germanaud, L.; Perchec, P. L. New Polymeric Phosphonato-, Phosphinato- and Carboxybetaines, 1. Syntheses and Characterization by IR Spectroscopy. *Makromol. Chem.* **1986**, *187*, 1097–1107.
- (11) Bonte, N.; Laschewsky, A. Zwitterionic Polymers with Carbobetaine Moieties. *Polymer* **1996**, *37*, 2011–2019.
- (12) Dupont, D.; Raiguel, S.; Binnemans, K. Sulfonic Acid Functionalized Ionic Liquids for Dissolution of Metal Oxides and Solvent Extraction of Metal Ions. *Chem. Commun.* **2015**, *51*, 9006–9009.
- (13) Reynolds, J. E.; Bohnsack, A. M.; Kristek, D. J.; Gutiérrez-Alejandre, A.; Dunning, S. G.; Waggoner, N. W.; Sikma, R. E.; Ibarra, I. A.; Humphrey, S. M. Phosphonium Zwitterions for Lighter and Chemically-Robust MOFs: Highly Reversible H2S Capture and Solvent-Triggered Release. J. Mater. Chem. A 2019, 7, 16842–16849.
- (14) Ai, L.; Ouyang, X.; Liu, Z.; Peng, R.; Jiang, W.; Li, W.; Zhang, L.; Hong, L.; Lei, T.; Guan, Q.; et al. Highly Efficient Polymer Solar Cells Using a Non-Conjugated Small-Molecule Zwitterion with Enhancement of Electron Transfer and Collection. *J. Mater. Chem. A* **2016**, *4*, 14944–14948.
- (15) Hemp, S. T.; Zhang, M.; Allen, M. H.; Cheng, S.; Moore, R. B.; Long, T. E. Comparing Ammonium and Phosphonium Polymerized Ionic Liquids: Thermal Analysis, Conductivity, and Morphology. *Macromol. Chem. Phys.* **2013**, *214*, 2099–2107.
- (16) Chen, M.; White, B. T.; Kasprzak, C. R.; Long, T. E. Advances in Phosphonium-Based Ionic Liquids and Poly(Ionic Liquid)s as Conductive Materials. *Eur. Polym. J.* **2018**, *108*, 28–37.
- (17) Zheng, L.; Sundaram, H. S.; Wei, Z.; Li, C.; Yuan, Z. Applications of Zwitterionic Polymers. In *Reactive and Functional Polymers*; Elsevier B.V., 2017; pp 51–61.
- (18) Sun, H.; Chang, M. Y. Z.; Cheng, W.-I.; Wang, Q.; Commisso, A.; Capeling, M.; Wu, Y.; Cheng, C. Biodegradable Zwitterionic Sulfobetaine Polymer and Its Conjugate with Paclitaxel for Sustained Drug Delivery. *Acta Biomater.* **2017**, *64*, 290–300.
- (19) Tan, H.; Liu, J.; Li, J.; Jiang, X.; Xie, X.; Zhong, Y.; Fu, Q. Synthesis and Hemocompatibility of Biomembrane Mimicing Poly-(Carbonate Urethane)s Containing Fluorinated Alkyl Phosphatidylcholine Side Groups. *Biomacromolecules* **2006**, *7*, 2591–2599.
- (20) Jung, J.; Kim, H.; Ree, M. Self-Assembly of Novel Lipid-Mimicking Brush Polymers in Nanoscale Thin Films. *Soft Matter* **2014**, *10*, 701–708.
- (21) Lowe, A. B.; McCormick, C. L. Synthesis and Solution Properties of Zwitterionic Polymers. *Chem. Rev.* **2002**, *102*, 4177–4190.
- (22) Georgiev, G. S.; Kamenska, E. B.; Vassileva, E. D.; Kamenova, I. P.; Georgieva, V. T.; Iliev, S. B.; Ivanov, I. A. Self-Assembly, Antipolyelectrolyte Effect, and Nonbiofouling Properties of Polyzwitterions. *Biomacromolecules* **2006**, *7*, 1329–1334.
- (23) Wu, T.; Beyer, F. L.; Brown, R. H.; Moore, R. B.; Long, T. E. Influence of Zwitterions on Thermomechanical Properties and Morphology of Acrylic Copolymers: Implications for Electroactive Applications. *Macromolecules* **2011**, *44*, 8056–8063.
- (24) Brown, R. H.; Duncan, A. J.; Choi, J.-H.; Park, J. K.; Wu, T.; Leo, D. J.; Winey, K. I.; Moore, R. B.; Long, T. E. Effect of Ionic Liquid on Mechanical Properties and Morphology of Zwitterionic Copolymer Membranes. *Macromolecules* **2010**, *43*, 790–796.
- (25) Kumar, R.; Fredrickson, G. H. Theory of Polyzwitterion Conformations. *J. Chem. Phys.* **2009**, *131*, No. 104901.

- (26) Bohrisch, J.; Schimmel, T.; Engelhardt, H.; Jaeger, W. Charge Interaction of Synthetic Polycarboxybetaines in Bulk and Solution. *Macromolecules* **2002**, *35*, 4143–4149.
- (27) Wang, R.; Lowe, A. B. RAFT Polymerization of Styrenic-Based Phosphonium Monomers and a New Family of Well-Defined Statistical and Block Polyampholytes. J. Polym. Sci., Part A: Polym. Chem. 2007, 45, 2468–2483.
- (28) Schultz, A. R.; Fahs, G. B.; Jangu, C.; Chen, M.; Moore, R. B.; Long, T. E. Phosphonium-Containing Diblock Copolymers from Living Anionic Polymerization of 4-Diphenylphosphino Styrene. *Chem. Commun.* **2016**, *52*, 950–953.
- (29) Jangu, C.; Schultz, A. R.; Wall, C. E.; Esker, A. R.; Long, T. E. Diphenylphosphino Styrene-Containing Homopolymers: Influence of Alkylation and Mobile Anions on Physical Properties. *Macromol. Rapid Commun.* **2016**, *37*, 1212–1217.
- (30) Schultz, A. R.; Chen, M.; Fahs, G. B.; Moore, R. B.; Long, T. E. Living Anionic Polymerization of 4-Diphenylphosphino Styrene for ABC Triblock Copolymers. *Polym. Int.* **2017**, *66*, 52–58.
- (31) Stewart, B.; Harriman, A.; Higham, L. J. Predicting the Air Stability of Phosphines. *Organometallics* **2011**, *30*, 5338–5343.
- (32) Paetzold, E.; Kinting, A.; Oehme, G. Synthesis of Phosphino Alkane Sulfonates and Their Corresponding Sulfonic Acids by Reaction of Alkalimetal-phosphides with Sultones. *J. Prakt. Chem.* 1987, 329, 725–731.
- (33) Romanov, S. R.; Aksunova, A. F.; Islamov, D. R.; Dobrynin, A. B.; Krivolapov, D. B.; Kataeva, O. N.; Bakhtiyarova, Y. V.; Gnezdilov, O. I.; Galkina, I. V.; Galkin, V. I. Triphenylphosphine in Reactions with ω-Haloalkylcarboxylic Acids. *Phosphorus, Sulfur Silicon Relat. Elem.* **2016**, 191, 1637–1639.
- (34) Wang, T.; Kou, R.; Liu, H.; Liu, L.; Zhang, G.; Liu, G. Anion Specificity of Polyzwitterionic Brushes with Different Carbon Spacer Lengths and Its Application for Controlling Protein Adsorption. *Langmuir* **2016**, *32*, 2698–2707.
- (35) Nwosu, C.; Coughlin, E. B. Pendant Side-Chain Sterics against Electrostatic Forces: Influencing Short-Range Ordering in Random Polyelectrolytes. *J. Polym. Sci., Part B: Polym. Phys.* **2019**, *57*, 1325–1336.
- (36) Chen, M.; Inglefield, D. L.; Zhang, K.; Hudson, A. G.; Talley, S. J.; Moore, R. B.; Long, T. E. Synthesis of Urea-Containing ABA Triblock Copolymers: Influence of Pendant Hydrogen Bonding on Morphology and Thermomechanical Properties. *J. Polym. Sci., Part A: Polym. Chem.* **2018**, *56*, 1844–1852.
- (37) Matsuura, H.; Eisenberg, A. Glass Transitions of Ethyl Acrylate-Based Ionomers. J. Polym. Sci., Polym. Phys. Ed. 1976, 14, 1201–1209.
- (38) Eisenberg, A.; Matsura, H.; Yokoyama, T. Glass Transition in Ionic Polymers: The Acrylates. *J. Polym. Sci., Part A-2: Polym. Phys.* 1971, 9, 2131–2135.
- (39) Tant, M. R.; Wilkes, G. L. An Overview of the Viscous and Viscoelastic Behavior of Ionomers in Bulk and Solution. *J. Macromol. Sci., Part C: Polym. Rev.* 1988, 28, 1–63.
- (40) Bocharova, V.; Wojnarowska, Z.; Cao, P.-F.; Fu, Y.; Kumar, R.; Li, B.; Novikov, V. N.; Zhao, S.; Kisliuk, A.; Saito, T.; et al. Influence of Chain Rigidity and Dielectric Constant on the Glass Transition Temperature in Polymerized Ionic Liquids. *J. Phys. Chem. B* **2017**, 121, 11511–11519.
- (41) Kumar, R.; Bocharova, V.; Strelcov, E.; Tselev, A.; Kravchenko, I. I.; Berdzinski, S.; Strehmel, V.; Ovchinnikova, O. S.; Minutolo, J. A.; Sangoro, J. R.; et al. Ion Transport and Softening in a Polymerized Ionic Liquid. *Nanoscale* **2015**, *7*, 947–955.
- (42) Fuoss, R. M.; Kraus, C. A. Properties of Electrolytic Solutions. III. The Dissociation Constant. *J. Am. Chem. Soc.* **1933**, *55*, 1019–1028.
- (43) Fuoss, F.; Accascina, R. M. Electrolytic Conductance; Interscience Publishers, Inc..: New York, NY, 1959.
- (44) Ebeling, W.; Grigo, M. An Analytical Calculation of the Equation of State and the Critical Point in a Dense Classical Fluid of Charged Hard Spheres. *Ann. Phys.* **1980**, *492*, 21–30.

- (45) Yokoyama, H.; Yamatera, H. A Theory of Ion Association as a Complement of the Debye-Hückel Theory. *Bull. Chem. Soc. Jpn.* **1975**, 48, 1770–1776.
- (46) Muthukumar, M. Localized Structures of Polymers with Longrange Interactions. *J. Chem. Phys.* **1996**, *104*, 691–700.
- (47) Schmuck, C.; Rehm, T.; Klein, K.; Gröhn, F. Formation of Vesicular Structures through the Self-Assembly of a Flexible Bis-Zwitterion in Dimethyl Sulfoxide. *Angew. Chem., Int. Ed.* **2007**, *46*, 1693–1697.
- (48) Bredas, J. L.; Chance, R. R.; Silbey, R. Head-Head Interactions in Zwitterionic Associating Polymers. *Macromolecules* **1988**, *21*, 1633–1639.
- (49) Middleton, L. R.; Trigg, E. B.; Yan, L.; Winey, K. I. Deformation-Induced Morphology Evolution of Precise Polyethylene Ionomers. *Polymer* **2018**, *144*, 184–191.
- (50) Kumar, R.; Lokitz, B.; Long, T. E.; Sumpter, B. G. Enhanced Scattering Induced by Electrostatic Correlations in Concentrated Solutions of Salt-Free Dipolar and Ionic Polymers. *J. Chem. Phys.* **2018**, *149*, No. 163336.
- (51) Kinning, D. J.; Thomas, E. L. Hard-Sphere Interactions between Spherical Domains in Diblock Copolymers. *Macromolecules* **1984**, *17*, 1712–1718.
- (52) Zhou, N. C.; Chan, C. D.; Winey, K. I. Reconciling STEM and X-Ray Scattering Data To Determine the Nanoscale Ionic Aggregate Morphology in Sulfonated Polystyrene Ionomers. *Macromolecules* **2008**, *41*, 6134–6140.
- (53) Ayyagari, C.; Bedrov, D.; Smith, G. D. Structure of Atactic Polystyrene: A Molecular Dynamics Simulation Study. *Macromolecules* **2000**, 33, 6194–6199.
- (54) Kirkwood, J. G. The Dielectric Polarization of Polar Liquids. *J. Chem. Phys.* **1939**, *7*, 911–919.
- (55) Onsager, L. Electric Moments of Molecules in Liquids. *J. Am. Chem. Soc.* **1936**, *58*, 1486–1493.
- (56) Zhang, C.; Hutter, J.; Sprik, M. Computing the Kirkwood G-Factor by Combining Constant Maxwell Electric Field and Electric Displacement Simulations: Application to the Dielectric Constant of Liquid Water. *J. Phys. Chem. Lett.* **2016**, *7*, 2696–2701.
- (57) Wypych, G. Handbook of Polymers, 2nd ed.; ChemTec Publishing: Toronto, 2016.
- (58) Bolt, H. M.; Golka, K. 1,3-Propane Sultone as an Extremely Potent Human Carcinogen: Description of an Exposed Cohort in Germany. J. Toxicol. Environ. Health, Part A 2012, 75, 544-550.
- (59) Zhang, F.; Ilavsky, J.; Long, G. G.; Quintana, J. P. G.; Allen, A. J.; Jemian, P. R. Glassy Carbon as an Absolute Intensity Calibration Standard for Small-Angle Scattering. *Metall. Mater. Trans. A* **2010**, *41*, 1151–1158.